AIAA JOURNAL
Vol. 50, No. 4, April 2012

Technical Notes

Simulation of Microgravity Diffusion Flames Using Sub-Atmospheric Pressures

Natalie Panek,* Marc R. J. Charest,* and Ömer L. Gülder†
University of Toronto, Toronto, Ontario M3H 5T6, Canada

DOI: 10.2514/1.J051306

I. Introduction

THE subject of combustion in weakly buoyant or microgravity environments has become a prominent branch of combustion science and research. Although understanding combustion will help to decrease particulate emissions and pollution from combustion technology used in earth-based applications, the future of space exploration depends on the safety of space technology, which includes a complete understanding of combustion processes in weakly buoyant environments. Combustion research in this area is essential for improving spacecraft safety for space missions and is also indispensable for gaining an in-depth understanding of combustion processes on earth. Without buoyant effects, novel flame behaviors are revealed [1]. A less common method to simulate weakly buoyant conditions is through subatmospheric pressures. At low pressures (pressures ranging from atmospheric down to near vacuum), the effects of buoyancy can be minimized during combustion. As a result, the characteristic residence times for combustion are slightly longer than under buoyant conditions [2].

Many flame properties during combustion are affected by a lack of buoyancy during the process. These properties of the laminar diffusion flames include but are not limited to soot formation processes, flame temperatures, flame dimensions, and flame stability and attachment mechanisms.

The formation and emission of soot in flames has been a long-standing research topic among scientists and engineers. Soot formation has been studied extensively at both atmospheric pressures and at high pressures; however, studies of soot at subatmospheric pressures are relatively limited. Experiments at high pressures are necessary to simulate the operational pressure range of most practical combustion technology. Results have shown that increases in pressure cause an increase in the concentration of soot formed in the flames [2–7]. Under the Earth's gravitational environment, buoyancy increases the axial velocities of the combustion species with increasing distance from the jet exit. The particles at the flame tip have the highest velocities because buoyancy has accelerated the particles over the largest distance [8]. Contrary to this, the absence of buoyancy tends to slow down the axial velocities of combustion species, albeit by a small amount, which increases the combustion residence time [2]. The longer residence times contribute to larger soot volume fractions and particle sizes as compared with soot production under normal gravity conditions [9]. Nonbuoyant diffusion flames also exhibit much broader soot-containing regions and larger soot-oxidation regions [10].

Studies regarding the shapes of nonbuoyant laminar jet diffusion flames in air have shown that these flames are longer than the buoyant flames resulting from a decrease in reactant mixing that occurs when buoyancy and gravitational effects are not involved in the reaction process [11]. Flames are also generally wider in microgravity than in normal gravity [12,13].

Some of the most common and widely used methods for simulating microgravity include drop towers, aircraft flying parabolic trajectories, sounding rockets, and spacecraft. An additional, however, less common, method to simulate nonbuoyant conditions is through subatmospheric pressures. At low pressures (pressures ranging from atmospheric down to near vacuum), the effects of buoyancy can be minimized during combustion. As a result, the characteristic residence times for combustion are longer than under buoyant conditions. These results must be interpreted with caution when comparing them with microgravity results because the vacuum environment is not isolated from the effects of gravity, only the effects of buoyancy.

The objective of this study was to investigate laminar ethylene/air diffusion flames at sub- and superatmospheric pressures to understand the effects of pressure and buoyancy on flame structure and soot formation. The physical flame appearance as well as the sooting characteristics and temperature field of the flames as affected by pressure were studied.

II. Experimental Methodology

Experiments were conducted in a combustion chamber [5,7] capable of operating at sub- and superatmospheric pressures with an inner diameter of 0.24 m and a height of 0.60 m. The details of the combustion chamber and the laminar coflow diffusion flame burner used in this study are reported in previous publications [5,7]. To generate low pressures for the current diffusion flame experiments, a vacuum pump was used in conjunction with a controller and a proportioning valve. The necessity for a continuous flow of air and fuel into the chamber during the flame experiments requires the vacuum pump to run continuously to sustain the pressure levels necessary for the duration of each experiment. Constant ethylene mass flow rates of 0.48 or 1.16 mg/s were used. The thermal-based mass flow meter is calibrated for low and high pressure uses and has a maximum total error of less than 2%. In all experiments, a coflow air flow rate of 0.11 g/s was used. The fuel nozzle of the burner is 3 mm in diameter, and the coflow air nozzle has a diameter of 25 mm.

A nonintrusive, line-of-sight spectral soot emission (SSE) diagnostic technique was used to obtain the temperature and the soot-volume fraction. In an SSE diagnostic, line-of-sight radiation emissions from soot are measured along chords through the flame at a given height. Soot emission is measured over the wavelength range of 690–945 nm. Spectra are averaged over the height of the entrance slit as well as across 12 spectral regions, each 21 nm wide. This provides 12 adjacent spectral data points per line-of-sight acquisition. Output from the spectrometer is focused onto a calibrated 16-bit charge-coupled device detector (1100×330 pixels). The lateral emission scans are inverted to obtain radially resolved emission data using the three-point Abel deconvolution technique, where the temperature and soot-volume fraction can be determined when soot optical properties are known [14]. Soot radiation emissions are measured every 50 μm across the flame at the height increments of 0.5 mm. Details of the theory are provided elsewhere [15], and the specifics of the overall experimental layout of the spectral soot

Presented as Paper 2010-1477 at the 48th AIAA Aerospace Sciences Meeting Including the New Horizons Forum and Aerospace Exposition, Orlando, Florida, 4–7 January 2010; received 29 March 2011; revision received 28 October 2011; accepted for publication 10 November 2011.

*Graduate Student, Institute for Aerospace Studies, 4925 Dufferin Street.
†Professor, Institute for Aerospace Studies, 4925 Dufferin Street; ogulder@utias.utoronto.ca. AIAA Associate Fellow (Corresponding Author).

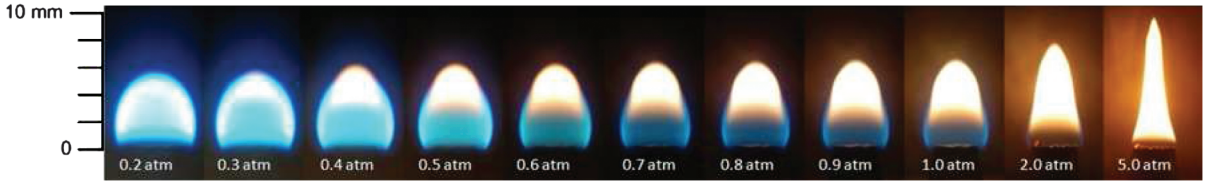

Fig. 1 Still pictures showing the shapes of laminar ethylene diffusion flames from 0.2 atm to 5 atm. The ethylene flow rate is 0.48 mg/s. The aperture and exposure time are adjusted to prevent image saturation from highly luminous flames. Flames were steady with a maximum change, due to flickering, in flame height less than 5%.

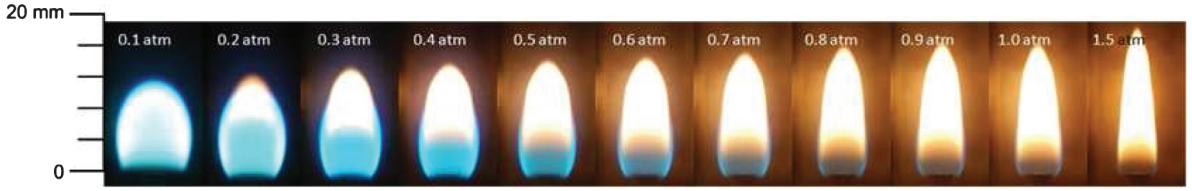

Fig. 2 Still pictures showing the shapes of laminar ethylene diffusion flames from 0.1 atm to 1.5 atm. The ethylene flow rate is 1.16 mg/s. The aperture and exposure time are adjusted to prevent image saturation from highly luminous flames. Flames were steady with a maximum change, due to flickering, in flame height less than 5%.

emission diagnostic used in this study are provided by Joo and Gülder [7].

III. Results and Discussion

At the flow rate of 0.48 mg/s ethylene, the measurements were taken at pressures from 0.2 atm to 5 atm. As the combustion chamber was evacuated down to 0.2 atm from atmospheric conditions, the flame became almost spherical with little or no soot production, as shown in Fig. 1. The flame at 0.2 atm no longer had a yellow luminous flame zone and became entirely blue, as seen at the far left of Fig. 1. The visible flame height, marked by the luminous flame zone or the visible blue flame boundary, decreased in height and significantly increased in width as the pressure is decreased at superatmospheric pressures, whereas it appeared to achieve a relatively constant height at the subatmospheric pressures down to 0.3 atm when the flame became almost spherical. (The stoichiometric flame height is expected to be constant for all pressures as a consequence of the proportionalities between volumetric flow rate, diffusivity, and pressure [16]).

At the higher ethylene flow rate of 1.16 mg/s, flame geometry variation was similar to the lower fuel flow rate flames. For this flow rate, the pressure range was from 0.1 atm to 1.5 atm, as shown in Fig. 2. At an ethylene flow rate of 0.48 mg/s, it was not possible to sustain a flame at 0.1 atm. For flow rate of 1.16 mg/s, the maximum pressure was 1.5 atm beyond which the flame became a smoking one and soot was escaping from the tip of the flame. The flames increased in width and decreased in height as the pressure decreased. At 0.1 atm pressure, the flame became completely blue and almost spherical, as seen in Fig. 2.

Soot volume fraction profiles at 0.5, 0.8, 1, and 2 atm at various flame height locations are shown in Figs. 3–6. Soot first nucleated in an annular ring towards the outer edges of the flame and transported inwards towards the flame centerline about halfway up the flame height before the soot was oxidized. Given all subatmospheric experimental conditions, as the pressure decreased, the soot volume fraction also decreased. At 1 atm, the maximum soot volume fraction was about 0.93 ppm, whereas at 0.5 atm, the soot volume fraction was negligible at about 0.08 ppm. As expected, the higher pressure flames produced even larger soot volume fractions and reached almost 6 ppm at 2 atm and about 60 ppm at 5 atm. The maximum soot-volume fraction profiles at various pressures and flame height locations are shown in Fig. 7 for the ethylene flow rate of 0.48 mg/s.

The peak soot-volume fraction was located at a height of between 4.5 mm and 5.5 mm at all pressures. In all cases, the soot volume fraction increased until this height and then decreased until the flame tip is reached. However, as the pressure decreased, the height at which soot could first be measured within the flame also moved towards the tip. This resulted in a much smaller range of heights over which soot was formed in the flame. At 1 atm, soot first began to form at 3 mm above the burner, whereas at 0.5 atm, soot first began to form at 4 mm above the burner tip.

To assess the sensitivity of sooting propensity of the flame to pressure, previous studies [5–7] suggested that the percentage of total

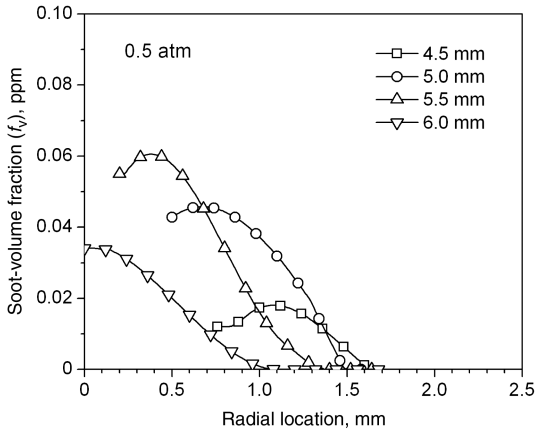

Fig. 3 Radial soot-volume fraction profiles at 0.5 atm. Ethylene flow rate 0.48 mg/s.

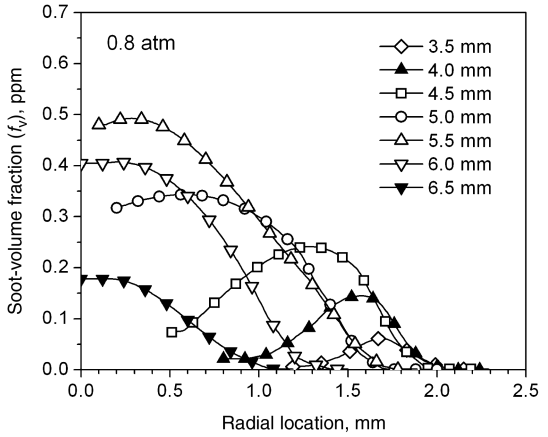

Fig. 4 Radial soot-volume fraction profiles at 0.8 atm. Ethylene flow rate 0.48 mg/s.

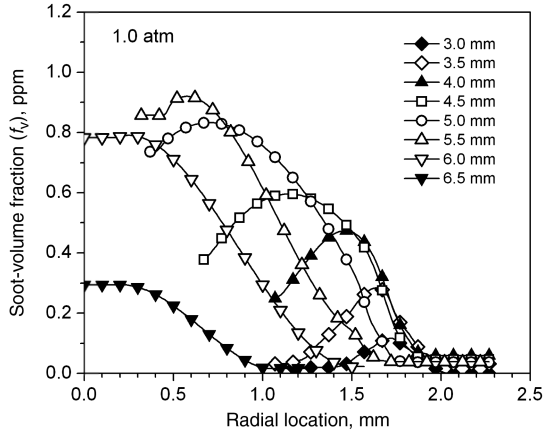

Fig. 5 Radial soot-volume fraction profiles at 1 atm. Ethylene flow rate 0.48 mg/s.

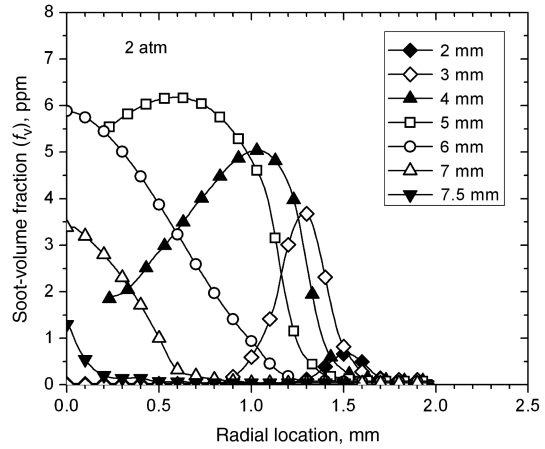

Fig. 6 Radial soot-volume fraction profiles at 2 atm. Ethylene flow rate 0.48 mg/s.

carbon in the fuel converted to soot as a function of height is a better measure than the maximum line-of-sight integrated soot concentrations. We use the same approach here to assess the influence of pressure. The mass flow rate of carbon, in the form of soot, can be determined through the relationship

$$\dot{m}_s(z) = 2\pi\rho_s \int v_z(r,z) f_v(r,z) r\,\mathrm{d}r \tag{1}$$

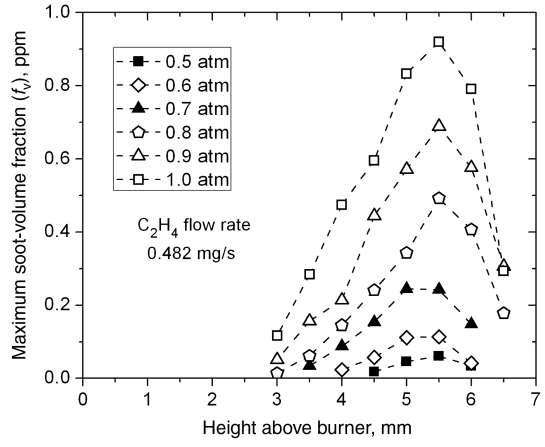

Fig. 7 Maximum soot-volume fractions as a function of height above the burner rim at various pressures.

where v_z is the axial velocity, $\rho_s = 1.8$ g/cm^3 is the soot density, and z is the axial height. The axial velocity could be estimated using the relationship $v_z(z) \approx \sqrt{2az}$, where a is an acceleration constant commonly assumed to be 25 m/s^2 at atmospheric pressure [16]. However, at subatmospheric pressures, assuming weakly buoyant conditions, the acceleration is found to vary with the square of the pressure [8]; that is the acceleration at subatmospheric conditions is assumed to be $a_s \approx aP^2$, where P is the pressure in atmospheres. The percentage of carbon in the fuel converted to soot is simply $\eta_s = \dot{m}_s/\dot{m}_c$, where $\dot{m}_c$ is the carbon mass flow rate at the nozzle exit.

A plot of maximum percentage conversion of carbon to soot at various heights along the flame axis, calculated using the approximate relationships described in the preceding paragraph, as a function of pressure is shown in Fig. 8 as a logarithmic plot. In recent studies [2,17,18], it was found that the acceleration constant a, which is used to estimate the axial velocity of the flame as a function of height, is larger than 25 m/s^2 at superatmospheric pressures. Also, at subatmospheric pressures, acceleration a_s exceeds the approximation given by $a_s \approx aP^2$. Instead of calculating the soot yield from Eq. (1) using the constant acceleration, the velocity field within the flame envelope computed from a full numerical simulation was used [17]. With this approach, the maximum carbon conversions to soot were systematically higher, as shown in Fig. 8. In Fig. 8, a power-law relationship between the percentage conversion of fuel's carbon to soot and the pressure is not obvious. However, if one seeks a relationship in the form of $\eta_s \propto P^n$, the value of exponent n is about 4.5 for the subatmospheric conversion rates for the fuel flow rate of 048 mg/s. Similar results were obtained for the higher flow rate of 1.16 mg/s (Fig. 8).

The most apparent discrepancy between microgravity and subatmospheric pressure results is that, as the pressure decreased from atmospheric to a near vacuum, the flame decreased in length and grew wider. Microgravity experiments indicate that diffusion flames should, in fact, increase in both length and width [19]. However, flames in both environments eventually formed a spherical, bulbous flame after continued exposure to a nonbuoyant environment.

The results from Urban et al. [20] for nonbuoyant, round, laminar jet diffusion flames show that the soot formation nucleates in the annular regions of the flame but that the peaks progress outwards at locations higher above the burner rim before starting to move inwards. As a result, the soot-volume fraction profiles become broader near the flame tip. This is opposite from the results in these experiments, which show that the soot peaks move inwards towards the flame centerline at increasing heights above the burner. However, the effects of burner nozzle diameter (larger in current experiments) and fuel flow rate (smaller in the current experiments) may also contribute to the observed soot profiles.

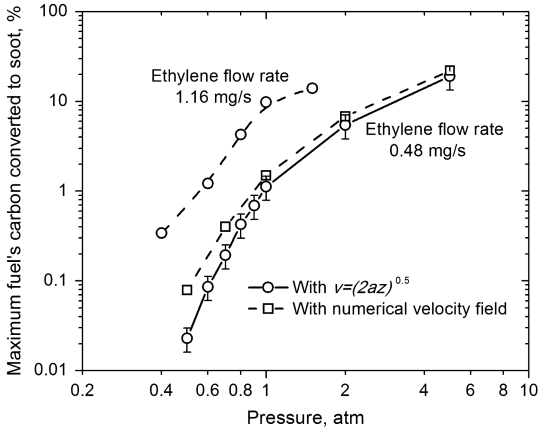

Fig. 8 Maximum fraction of fuel's carbon converted to soot on a logarithmic scale. The average slope of the subatmospheric portion of the curve evaluated using the computed velocity field is about 4.5 for an ethylene flow rate of 0.48 mg/s.

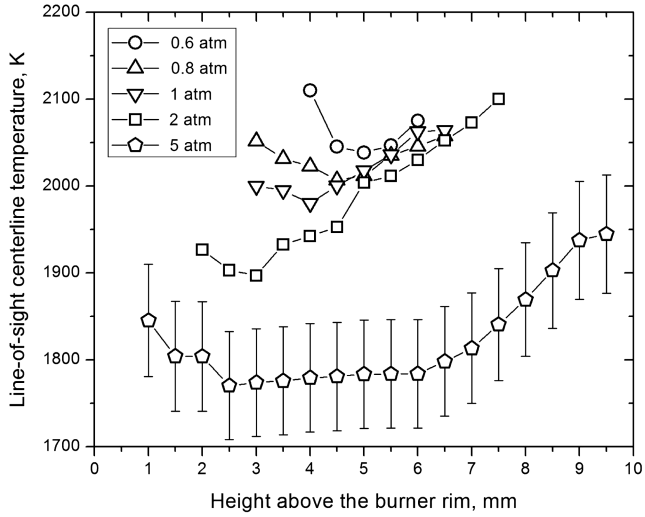

Fig. 9 Line-of-sight centerline flame temperatures at various pressures as a function of height above the burner rim. Ethylene flow rate 0.48 mg/s.

The apparent difference between results is due to an increase in both flame length and width in microgravity, whereas there is only an increase in flame width at subatmospheric pressures. Because the flame decreases in size, the soot-volume fraction profiles of subatmospheric flames must, therefore, move inwards to the flame centerline. These results are consistent with flame temperatures in each environment because flame temperature has a direct relationship with the amount of soot formed in the flame. Because less soot is formed in a near vacuum than in microgravity, the flame temperatures are expected to be higher due to less soot radiation. The measured line-of-sight centerline flame temperatures, which are expected to represent an overall temperature, are shown in Fig. 9. The temperatures are reduced as the pressure goes from 0.5 atm to the atmospheric as expected. Current results cannot be directly compared with previous studies at subatmospheric pressures [21,22] in which the effect of pressure was not systematically investigated and fuel flow rates were much higher than the those in the current study.

It should be noted that the soot volume fractions measured at subatmospheric pressures in the present study are almost tenfold smaller than soot-volume fractions measured under microgravity conditions [8]. At subatmospheric pressures, only partial effects of microgravity could be realized. For example, combustion intensity (energy release per unit volume) roughly scales with the square of the pressure; as a consequence of this, combustion reactions are expected to be slower at low pressures. This could be remedied to a certain extent by using pure oxygen instead of air.

The locations of the peak soot-volume fraction at each pressure level also indicate that the soot nucleated at larger radial locations for the subatmospheric pressures as compared with the superatmospheric pressures. However, the differences in the width of the flames at the subatmospheric pressures are negligible, as is evident by the consistent location of the peak soot-volume fraction profiles from the flame centerline at each height between 0.5 and 1 atm, as shown in Fig. 7.

Total uncertainties for soot and temperature measurements were estimated as 35% and 3.5%, respectively. Sources of these uncertainties are detailed in previous publications [5–7]. Error bars in Figs. 8 and 9 reflect these uncertainties.

IV. Conclusions

Unlike nonbuoyant flames generated in microgravity facilities, low-pressure flames have lower soot-volume fractions. Although the results from the near-vacuum measurements are consistent with the trends from high pressure combustion experiments, they are not consistent with results recorded from diffusion flame experiments in drop towers, flights aboard parabolic aircraft, or aboard the International Space Station. The main conclusions can be summarized as follows:

1) It is evident that factors, aside from low buoyancy, are present during microgravity combustion, which may not be fully captured using subatmospheric flames.

2) Sensitivity of soot formation to pressure is not the same at subatmospheric and superatmospheric pressures. At subatmospheric conditions, soot formation shows a very strong dependence on pressure; this dependence gets weaker as the pressure is increased.

3) For the small flames used in this study, acceleration approximations based one one-dimensional arguments yield significant errors in carbon conversion to soot evaluations.

Acknowledgment

Operational funds for this work have been provided by the Natural Sciences and Engineering Research Council and Canadian Space Agency.

References

[1] Ross, H. D., "Basics of Microgravity Combustion," *Microgravity Combustion: Fire in Freefall*, edited by H. D. Ross, Academic Press, New York/London/Orlando, FL, 2001, pp. 1–33.

[2] Charest, M. R. J., Groth, C. P. T., and Gülder, Ö. L., "A Numerical Study on the Effects of Pressure and Gravity in Laminar Ethylene Diffusion Flames," *Combustion and Flame*, Vol. 158, 2011, pp. 1933–1945. doi:10.1016/j.combustflame.2011.02.022

[3] Lee, W., and Na, Y. D., "Soot Study in Laminar Diffusion Flames at Elevated Pressure Using Two-Color Pyrometry and Abel Inversion," *JSME International Journal Series B: Fluids and Thermal Engineering*, Vol. 43, No. 4, 2000, pp. 550–555.

[4] McCrain, L. L., and Roberts, W. L., "Measurements of the Soot Volume Field in Laminar Diffusion Flames at Elevated Pressures," *Combustion and Flame*, Vol. 140, 2005, pp. 60–69. doi:10.1016/j.combustflame.2004.10.005

[5] Thomson, K. A., Gülder, Ö. L., Weckman, E. J., Fraser, R. A., Smallwood, G. J., and Snelling, D. R., "Soot Concentration and Temperature Measurements in Co-annular, Non-Premixed CH4/Air Laminar Flames at Pressures up to 4 MPa," *Combustion and Flame*, Vol. 140, 2005, pp. 222–232. doi:10.1016/j.combustflame.2004.11.012

[6] Bento, D. S., Thomson, K. A., and Gülder, Ö. L., "Soot Formation and Temperature Field Structure in Laminar Propane-air Diffusion Flames at Elevated Pressures", *Combustion and Flame*, Vol. 145, 2006, pp. 765–778. doi:10.1016/j.combustflame.2006.01.010

[7] Joo, H. I., and Gülder, Ö. L., "Soot Formation and Temperature Field Structure in Coflow Laminar Diffusion Flames at Pressures from 10 to 60 Atmospheres," *Proceedings of the Combustion Institute*, Vol. 32, 2009, pp. 769–775. doi:10.1016/j.proci.2008.06.166

[8] Law, C. K., and Faeth, G. M., "Opportunities and Challenges of Combustion in Micro-Gravity," *Progress in Energy and Combustion Science*, Vol. 20, No. 1, 1994, pp. 65–113. doi:10.1016/0360-1285(94)90006-X

[9] Ku, J. C., Griffin, D. W., Greenberg, P. S., and Roma, J., "Buoyancy-Induced Differences in Soot Morphology," *Combustion and Flame*, Vol. 102, Nos. 1–2, July 1995, pp. 216–218. doi:10.1016/0010-2180(95)00108-I

[10] Kaplan, C. R., Oran, E. S., Kailasanath, K., and Ross, H. D., "Gravitational Effects on Sooting Diffusion Flames," *Proceedings of the Combustion Institute*, Vol. 26, No. 1, 1996, pp. 1301–1309.

[11] Lin, K. C., Faeth, G. M., Sunderland, P. B., Urban, D. L., and Yuan, Z. G., "Shapes of Non-Buoyant Round Luminous Hydrocarbon/Air Laminar Jet Diffusion Flames," *Combustion and Flame*, Vol. 116, No. 3, 1999, pp. 415–431.

[12] Berlad, A. L., Huggett, C., Kaufman, F., Markstein, G. H., Palmer, H. B., and Yang, C. H., "Study of Combustion Experiments in Space," NASA Rept. CR-134744, 1974.

[13] Edelman, R. B., Fortune, O., and Weilerstein, G., "Analytical Study of Gravity Effects on Laminar Diffusion Flames," NASA Report No. NASA-CR-120921, 1972.

[14] Dasch, C. J., "One-Dimensional Tomography: A Comparison of Abel, Onion-Peeling, and Filtered Backprojection Methods," *Applied Optics*, Vol. 31, No. 8, 1992, pp. 1146–1152.

doi:10.1364/AO.31.001146
[15] Snelling, D. R., Thomson, K. A., Smallwood, G. J., Gülder, Ö. L., Weckman, E. J., and Fraser, R. A., "Spectrally Resolved Measurement of Flame Radiation to Determine Soot Temperature and Concentration," *AIAA Journal*, Vol. 40, No. 9, 2002, pp. 1789–1795. doi:10.2514/2.1855
[16] Roper, F. G., Smith, C., and Cunningham, A. C., "The Prediction of Laminar Jet Diffusion Flame Sizes. II. Experimental Verification," *Combustion and Flame*, Vol. 29 No. 3, 1977, pp. 227–234. doi:10.1016/0010-2180(77)90113-4
[17] Charest, M. R. J., Groth,C. P. T., and Gülder, Ö. L., "A Numerical Study on Effects of Pressure and Gravity in Laminar Ethylene Diffusion Flames," *Combustion and Flame*, Vol. 158, 2011, pp. 1933–4545. doi:10.1016/j.combustflame.2011.02.022
[18] Gülder, Ö. L., Intasopa, G., Joo, H. I., Mandatori, P. M., Bento, D. S., and Vaillancourt, M. E., "Unified Behaviour of Maximum Soot Yields of Methane, Ethane and Propane Laminar Diffusion Flames at High Pressures," *Combustion and Flame*, Vol. 158, 2011, pp. 2037–2044. doi:10.1016/j.combustflame.2011.03.010
[19] *Proceedings of the 7th International Workshop on Microgravity Combustion and Chemically Reacting Systems*, NASA TR NASA/CP 212376/REV1, 2003.
[20] Urban, D. L., Yuan, Z. G., Sunderland, P. B., Linteris, G. T., Voss, J. E., Lin, K. C., Dai, Z., Sun, K., and Faeth, G. M., "Structure and Soot Properties of Non-buoyant Ethylene/Air Laminar Jet Diffusion Flames," *AIAA Journal*, Vol. 36 No. 8, 1998, pp. 1346–1360. doi:10.2514/2.542
[21] Sunderland, P. B., and Faeth, G. M., "Soot Formation in Hydrocarbon/Air Laminar Jet Diffusion Flames," *Combustion and Flame*, Vol. 105, 1996, pp. 132–146. doi:10.1016/0010-2180(95)00182-4
[22] Sunderland, P. B., Köylü, Ü. Ö., and Faeth, G. M., "Soot Formation in Weakly-Buoyant Acetylene-Fueled Laminar Jet Diffusion Flames Burning in Air," *Combustion and Flame*, Vol. 100, 1995, pp. 310–322. doi:10.1016/0010-2180(94)00137-H

J. Drummond
Associate Editor